RSC Advances

PAPER

View Article Online
View Journal | View Issue

Cite this: *RSC Adv.*, 2026, **16**, 24667

Paper-based electrochemical sensor for direct detection of caffeine in commercial beverage samples

Muhammad Yudha Syahputra, [a] Erika Shinchi, [b] Kenji Shida[c] and Masato Tominaga *[a]

Paper-based sensors offer a promising route toward portable and biodegradable electrochemical sensors for microvolume analysis; however, their application to the detection of caffeine remains limited. In this study, we developed a paper-based electrochemical sensor for direct detection of caffeine in commercial beverages without sample pretreatment. The sensor was fabricated by integrating multi-walled carbon nanotubes (MWCNTs) onto wax-modified paper supported by a cellulose nanofibre (CNF) film. Electrochemical investigations revealed an irreversible caffeine oxidation current at the MWCNTs-modified electrode, which was due to a diffusion-controlled reaction. The caffeine oxidation reaction was found to proceed through a two-proton, four-electron transfer mechanism, as determined by the potential peak shift and caffeine diffusion coefficient. The sensor enabled direct detection of caffeine in microvolume samples and was successfully applied to commercial beverages without any pretreatment. Square wave voltammetry demonstrated sensitive and selective caffeine detection with a linear response over a caffeine concentration range of 5–200 μM. Reliable caffeine quantification was achieved using only 20 μL of sample, with measured caffeine concentrations consistent with those obtained by liquid chromatography-mass spectrometry. These results demonstrate the potential of the developed paper-based sensor as a sustainable and practical platform for the direct electrochemical analysis of caffeine in beverages.

Received 6th February 2026
Accepted 3rd May 2026

DOI: 10.1039/d6ra01066k

rsc.li/rsc-advances

1. Introduction

Caffeine (1,3,7-trimethylxanthine) is a natural alkaloid commonly found in beverages such as tea, coffee, chocolate, and energy drinks.[1] However, long-term consumption of caffeine may lead to addiction, insomnia, or other adverse effects. Excessive caffeine consumption also causes poor sleep and decreased academic performance.[2] Therefore, children, teenagers, pregnant women, and people sensitive to caffeine are recommended to reduce their consumption of caffeine to lower the risk of its side effects.[3,4] However, beverage labels often provide only limited information regarding caffeine content, necessitating the development of fast, affordable, and user-friendly sensors for the determination of caffeine levels in beverages. Although various methods for the evaluation of caffeine concentrations are currently available, such as chromatographic[5–7] and spectroscopic[8–10] methods that provide excellent sensitivity for caffeine detection, they require complicated and time-consuming multistep sample pretreatments. Electrochemical methods provide a promising alternative to conventional caffeine detection methods by enabling simple, rapid and yet highly sensitive analysis using affordable instruments.[11,12] Caffeine molecules have been reported to be electrochemically active in acidic media in which caffeine is protonated to support its oxidation reaction.[13,14] Electrochemical oxidation of caffeine is an irreversible 4-electron and 4-proton reaction that oxidizes caffeine into 8-hydroxycaffeine (1,3,7-trimethyluric acid).[15,16] Recent reports on the electrochemical detection of caffeine have focused on modifications of glassy carbon electrodes and carbon paste electrodes with functional materials such as nanocarbon materials,[17–22] nanomaterials,[23–28] conductive polymers[29,30] and biomolecule materials[31–36] to improve sensor sensitivity and selectivity. However, despite advances in the development of electrochemical sensing of caffeine, the reported detection platforms still show limitations with regard to portability and simplicity, rendering them unsuitable for practical use in on-site measurements.

Recently, electrochemical paper-based analytical devices (ePAD) have been widely used for detection of health-related compounds in clinical settings and food monitoring. These devices are constructed through the application of conductive

[a]Graduate School of Science and Engineering, Saga University, 1 Honjomachi, Saga 840-8502, Japan. E-mail: masato@cc.saga-u.ac.jp
[b]Analytical Research Center for Experimental Science, Saga University, 1 Honjomachi, Saga 840-8502, Japan
[c]Faculty of Engineering, Kumamoto University, Kumamoto 860-8555, Japan

materials to form electrochemical cell.[37,38] The first ePAD was developed by Dungchai *et al.* (2009) who demonstrated the ability of paper integrated with carbon-ink-modified Prussian blue to determine glucose, lactate, and uric acid levels in serum samples.[37] Following this pioneering work, ePAD technology has been applied to the detection of various analytes, including drugs,[39] heavy metals,[40] and viruses[41,42] owing to its cost-effectiveness, portability, and capability for on-site analysis. However, to the best of our knowledge, ePADs have not been used for the determination of caffeine levels in commercial beverages. Therefore, this study introduces a new approach for the direct detection of caffeine content in beverage samples using an ePAD system. The paper surface was modified with wax using the scratch method to prepare a hydrophobic surface which inhibited the absorption of the sample solution into the paper layer. Multi-walled carbon nanotubes (MWCNTs) were integrated as the electrode material onto the wax-modified paper. Cellulose nanofibre (CNF) film was incorporated to connect the electrolyte and electrodes in the detection region. MWCNTs were selected as the working electrode because of their high electrical conductivity and large surface area.[43] In addition, CNF film is flexible and has good chemical stability.[44,45] CNF film as supporting matrix promotes uniform solution distribution across the electrode active surface. Polybenzimidazole (PBI) was used as dispersing agent for MWCNTs, PBI/MWCNT is used as counter electrode. The electrochemical behaviour of caffeine, including its diffusion characteristics and oxidation reaction mechanism, at the multiwalled carbon nanotube (MWCNTs)-modified electrode was investigated. The fabricated paper-based sensor was demonstrated to determine the caffeine concentration in commercial beverage samples without sample pretreatment. The determined caffeine concentrations of the commercial beverage samples were consistent with those evaluated by liquid chromatography-mass spectrometry (LC-MS) analysis.

2. Materials and methods

2.1 Materials

Whatman 1 CHR chromatography paper with a pore size of 11 μm was purchased from international company, UK. The Kiriyama wax candles were purchased from convenience stores. Nanoforest-S BB cellulose nanofiber (CNF) obtained from bamboo using an aqueous counter-collision method was purchased from Chuetsu Pulp and Paper Co., Ltd, Japan. MWCNTs (purity: > 98%, length 3–6 μm, outer diameter: 10 ± 1 nm, inner diameter: 4.5 ± 0.5 nm) were purchased from Sigma-Aldrich. Polybenzimidazole (PBI) powder was purchased from Sato Light Industrial Co., Ltd (Japan). *N*,*N*-dimethylacetamide (DMAc), sodium hydroxide (NaOH), and hydrochloric acid (HCl) were purchased from Fujifilm Wako Pure Chemicals. Briton & Robinson buffers were prepared by mixing boric acid (HBO_3), phosphoric acid (H_3PO_4) and acetic acid (CH_3COOH) (Fujifilm Wako Pure Chemical) and the buffer pH was adjusted using 0.1 M NaOH and 0.1 M HCl. All solutions were prepared using deionised water purified with a Milli-Q water purification system.

2.2 Fabrication of MWCNTs paper-based electrode

First, the Whatman chromatography paper was cut into 10 mm × 11 mm pieces. Then, wax was uniformly deposited onto the paper surface by gently scratching a Kameyama candle across the paper and subsequently melted by heating on a hotplate at 70 °C for 5 min to form a hydrophobic barrier. A three-electrode system was used to construct an electrochemical platform. First, a solution of dispersed MWCNTs was prepared by dispersing MWCNTs (8 mg) in water (10 mL) and homogenising it using probe ultrasonication for 20 min according to our previous work.[44,45] A dispersed solution of the PBI/MWCNTs was prepared as follows: first, PBI (40 mg) was dissolved in DMAc (10 mL) and sonicated for 20 min (the prepared solution is denoted as PBI/DMAC). Second, MWCNTs (6 mg) were mixed with DMAc (3 mL), and then PBI/DMAC (60 μL) was added. Finally, the mixed PBI–MWCNTs solution was sonicated for 20 min. The drop-cast method was used to prepare the three-electrode system for the sensor. To precisely control the casting area, masking method was employed to define fixed electrode geometry on the paper substrate. 50 μL of the dispersed MWCNTs was used as the working electrode, 2 μL of Ag/AgCl ink served as the reference electrode, and 50 μL of the dispersed PBI/MWCNTs solution was used as the counter electrode. The fabricated paper-based sensor was dried overnight at room temperature and was subjected to a UV-ozone treatment to remove surface contaminants. Finally, a CNF film was utilised to establish a channel connecting the electrolyte solution and the three electrodes on the wax-modified paper. The CNF film was prepared as follows: CNF (1 g) was dispersed in water (20 mL) by probe ultrasonication for 20 min. Then, the dispersed-CNF solution (10 mL) was spread onto a Teflon plate and heated at 140 °C on a hot plate. After film formation, the CNF film was carefully peeled from the Teflon plate. Finally, the obtained CNF film was cut into 3 × 11 mm^2 pieces for further use. The paper-based sensor is shown in Fig. 1.

2.3 Statistical analysis

The paper-based sensor measurement was performed in triplicate ($n = 3$), and the result were presented as mean ± standard deviation (SD). The interference study data were subjected to one-way ANOVA ($p < 0.05$) using Microsoft Excel data-analysis tool pack to evaluate the sensor selectivity.

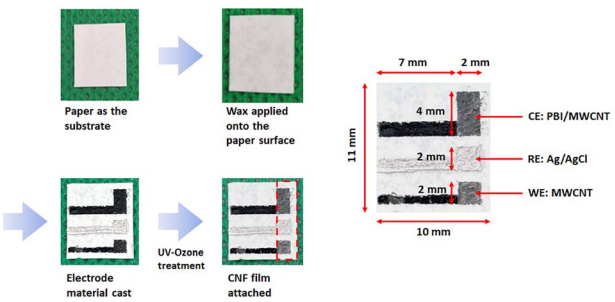

Fig. 1 Fabrication and design of the paper-based sensor with integrated three-electrode system.

2.4 Instrumentation

Scanning electron microscopy (SEM) images were obtained using a JSM-7609F microscope (JEOL, Japan). Prior to SEM measurements, each sample was coated with osmium (~5 nm) by sputtering. Dispersed solutions were prepared using a probe sonicator (BRANSON 5520, Japan). LC-MS measurements were performed using a SHIMADZU LCMS-8045 instrument with a Shim-pack XR-ODS II (SHIMADZU, Japan) as the column. The resistance of the paper-based sensor was evaluated by electrochemical impedance spectroscopy (EIS) using an electrochemical analyser (HZ-Pro S4, HOKUTO DENKO, Ltd, Japan). The impedance measurements were performed in a Faraday cage. The pH was evaluated using a pH meter AUT-501 (DKK-TOA Corp., Japan). Cyclic voltammetry (CV) and square wave voltammetry (SWV) were performed using an ALS CHI660A electrochemical analyser (ALS Co., Ltd, Japan). All electrochemical measurements were performed under ambient conditions.

3. Results and discussion

3.1 Paper-based electrode characterization

A solution-flow test was conducted to evaluate the solution distribution in the paper-based sensor (Fig. 2). The paper-based sensor with the applied wax and CNF film demonstrated an effective and uniform solution distribution within the desired electrode area of the sensor. The results clearly demonstrated the following effects of the wax and CNF films. First, the hydrophobic barrier formed by wax on the paper surface inhibits solution absorption into the paper layer. Second, the CNF film enabled a uniform distribution of the solution. Third, a uniform surface area for electrochemical measurements was established owing to the limited contact area of the electrode surface with the sample solution. These effects contributed to the repeatability of the sensing performance of the sensor. For instance, the Ag paste reference electrode exhibited stable potential for more than 10 min in a 0.1 M phosphate solution at pH 1 (Fig. S1). The conductivity of the paper-based sensor was evaluated using EIS measurements carried out using 1.0 mM $[Fe(CN)_6]^{3-}$ in a 1.0 M KCl solution. A high charge-transfer resistance (R_{CT}) was obtained from the Nyquist plots (514.5 ± 109.2 Ω, Fig. S2), indicating high resistance owing to the CNF film acting as a barrier between the solution and electrode surface. However, despite the relatively high resistance of the paper-based electrode, the couple of ferricyanide/ferrocyanide redox current was observed, confirming that the paper-based sensor functioned as an electrode (Fig. S4). The thin layer electrochemical diffusion behaviour was observed, this due to the porous properties of CNF film.[46] Additionally, well-defined peak current for caffeine oxidation was obtained by CV in a 0.1 M phosphate solution containing 1.0 mM caffeine (Fig. S5).

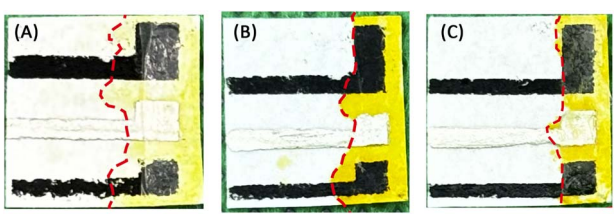

Fig. 2 Results of the flow test for the paper-based sensor (A) without wax, (B) with applied wax and without CNF film, and (C) with applied wax and CNF film.

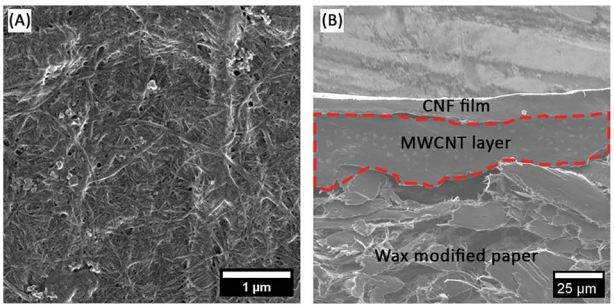

Fig. 3 SEM images of (A) surface and (B) cross-section of the MWCNTs modified paper-based sensor.

The SEM images showed the morphological features of the surface and the cross-section of the paper-based sensor (Fig. 3 (A) and (B)). A fibrous surface was observed for the CNF film; such a surface structure enables efficient retention and uniform distribution of the electrolyte across the electrode surface. Examination of the cross-sectional morphology revealed a laminated structure comprising wax-modified paper, an MWCNTs layer, and a thin layer of CNF film. The thin CNF-film layer was attached to the MWCNTs surface, enabling efficient solution distribution to the sensor surface. The thickness of the CNF film was estimated to be 12.2 μm. The MWCNTs layer (thickness of *ca.* 38.1 μm) underneath the CNF film acted as the conducting layer. The thickness of the overall paper-based sensor was determined to be 221 μm. The wax-modified paper used as the substrate supported the stable structure of the electrode and served as a hydrophobic barrier, facilitating the confinement of the solution in the defined electrode area. The observed multilayer configuration provided both mechanical stability and an efficient charge transport pathway across the electrode.

3.2 Electrochemical characteristics

To analyse the fundamental of electrochemical interaction between MWCNTs, caffeine and its environment, we performed CV measurements on the MWCNTs-modified glassy carbon electrode (GCE) in a phosphate solution electrolyte (pH 1) in the absence and presence of 1 mM caffeine with the obtained results shown in Fig. 4(A) by dashed and solid lines, respectively. As mentioned earlier, a well-defined oxidation current peak was observed at approximately +1.2 V (*vs.* Ag|AgCl|sat. KCl) and no reduction current was observed at the reverse potential, indicating the irreversibility of the caffeine oxidation reaction. This behaviour is similar to that observed in previous studies.[13,14]

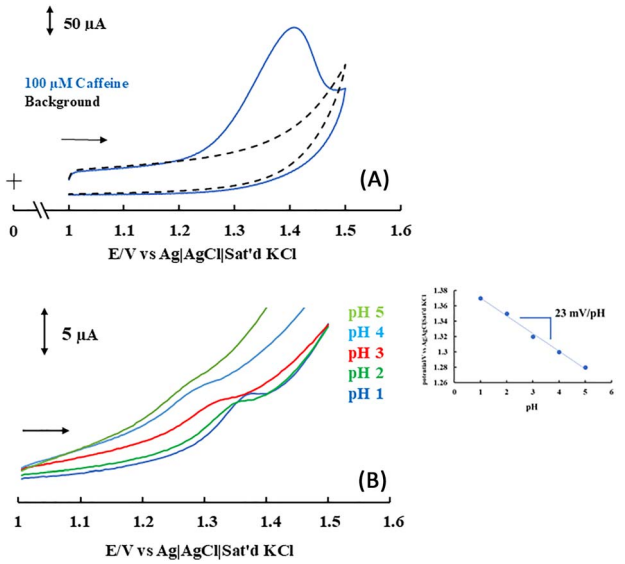

Fig. 4 CV results in 0.1 M phosphate solution at MWCNTs/GCE in the absence (dashed line) and presence (solid line) of 1 mM caffeine (A). Effect of pH on the oxidation current and peak potential of caffeine (B).

The effects of both pH and electrolyte species were investigated to optimise the measurement conditions for caffeine detection. The electrochemical behaviour of caffeine was strongly expected to be influenced by pH because the caffeine oxidation reaction included proton transfer. Therefore, the influence of pH was evaluated in the pH range of 1–5 (Fig. 4(B)). The peak potentials were observed to shift towards negative potentials with increasing pH. The plot of peak potential (E_p) *versus* pH (inset of Fig. 4(B)) showed a slope of −23 mV pH^{-1}. These results clearly indicated that the proton-to-electron ratio was 1 : 2. In particular, well-defined oxidation currents were observed at pH 1 and 2, indicating that caffeine oxidation was favourable under strongly acidic conditions, such as those obtained using H_3PO_4 and H_2SO_4. This result is consistent with previous studies in which phosphoric acid and sulfuric acid were used as electrolytes.[26,47–49] The effect of the electrolyte species was also investigated at pH 1 (Fig. 5). Interestingly, no caffeine oxidation current was observed in the presence of HCl, even in a strongly acidic solution (pH 1). By contrast, a clear current was observed for both H_3PO_4 and H_2SO_4 solutions. These results may be attributed to the mechanism of caffeine oxidation at the electrode surface. Moreover, the onset potential (at which the oxidation current begins to appear) was found to depend on the electrolyte solution (pH 1). In the phosphate solution, the onset potential was more negative than that in the sulphate solution, indicating that the phosphate solution provided better catalytic performance. Hence, phosphate solution was identified as the optimal electrolyte.

The electrochemical kinetics of caffeine were also studied by plotting the peak current obtained in CV measurements performed in the scan-rate range of 5–100 mVs^{-1} as a function of the square root of the scan rate. The obtained peak current slope exhibits a linear relationship with $v^{1/2}$ at high and low caffeine concentrations, indicating a diffusion-controlled reaction process (Fig. S7). Using the Randles–Sevcik equation, the diffusion coefficient (D) of caffeine was estimated as 5.36×10^{-6} $cm^2\ s^{-1}$ (eqn (1)). This value is in good agreement with the D values calculated by the Stokes–Einstein equation (eqn (2)) using the dimensions of the caffeine molecule, as shown in Fig. 6. The obtained D value was also in close agreement with the previously reported D values ($\sim 10^{-6}$ $cm^2\ s^{-1}$).[50–52]

$$i_p = \pm(2.69 \times 10^5) n^{\frac{3}{2}} A D^{\frac{1}{2}} C v^{\frac{1}{2}} \quad (1)$$

$$D = \frac{RT}{6\pi r \eta N} \quad (2)$$

The D value obtained with the Stokes–Einstein equation was used to determine the number of electrons involved in the caffeine oxidation reaction (n) using eqn (1), obtaining $n = 4$. The 1 : 2 ratio of protons to electrons derived from the potential

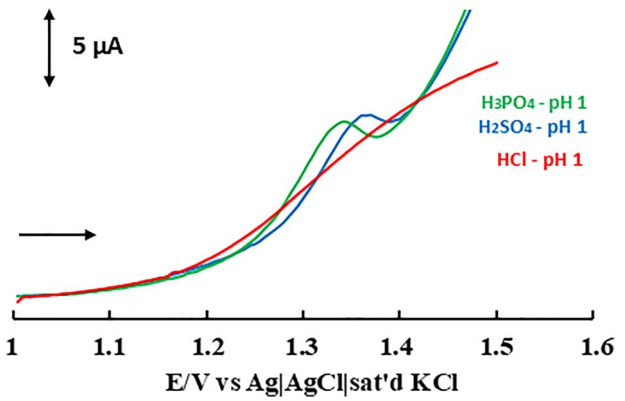

Fig. 5 Effect of electrolyte species on the oxidation current of caffeine.

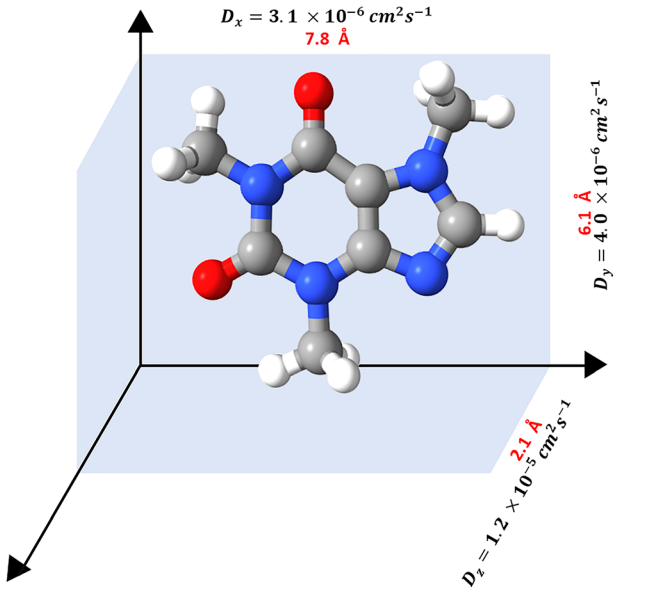

Fig. 6 Diffusion coefficient (D) calculated using the Stoke–Einstein equation based on the size of the caffeine molecule.[47]

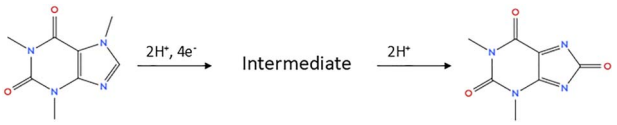

Fig. 7 Suggested caffeine oxidation reaction.

peak shift value indicates that 2 protons and 4 electrons are involved in the caffeine oxidation reaction, corresponding to the proton–electron ratio of 2 : 4 (Fig. 7). This ratio is different from the previously reported proton–electron ratio of 4 : 4;[15,16] this difference may be caused by the differences in the utilised electrode materials, electrode interface interactions and the electrolyte environment between the system used in our sensor and those used in previous studies.

3.3 Performance of paper-based sensor

Based on the fundamental understanding from the MWCNTs/GCE system, the paper-based sensor was subsequently developed to incorporate factors including pH effect, acid species and diffusion behaviour of caffeine into practical sensing platform. The SWV measurements were performed to investigate the practical performance of the paper-based sensor due to the reduced double-layer capacitance. The measurements were performed under optimised conditions in the phosphate solution (pH 1). The parameters of the measurements were as follows: initial potential (E_i) = 1 V, final potential (E_f) = 1.5 V, square-wave frequency = 1 Hz, amplitude = 20 mV, and potential step = 5 mV; the measurements were conducted using only 20 μL of the solution. According to the SWV results, the caffeine oxidation current was observed at 1.1 V and the peak current was observed at *ca.* +1.27 V (Fig. 8). The oxidation peak current value increased proportionally with increasing caffeine concentration, and linear responses were produced for concentrations ranging from 5 to 200 μM ($y = 2.52\times$; $R^2 = 0.9991$). The detection range of the paper-based sensor was comparable to those of the bare GCE and unmodified screen-printed electrodes (SPE) while achieving lower limit of detection (Table 1). In comparison with sensors developed in previous studies, the prepared paper-based sensor provides the advantages of disposability for one-time use and low sample consumption (20 μL).

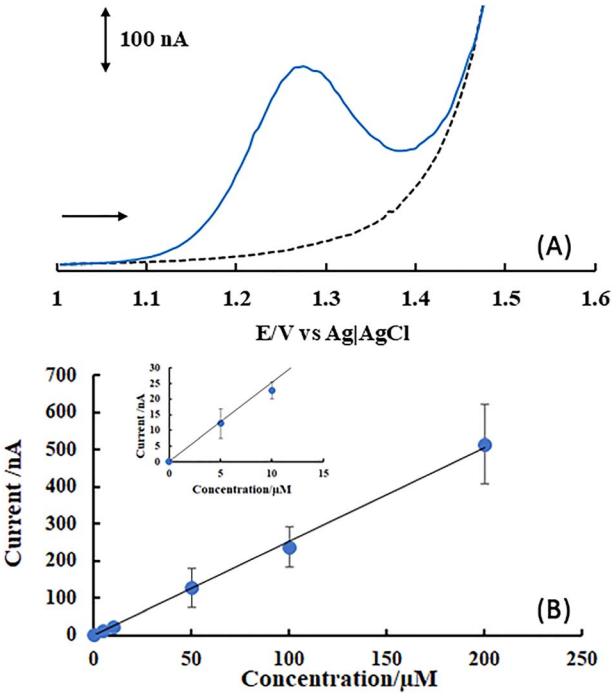

Fig. 8 SWV results for caffeine detection in 0.1 M phosphate solution at the paper-based sensor (A); current as a function of concentration for caffeine detection in 0.1 M phosphate solution (B).

Table 1 Comparison of the analytical performance obtained with carbon electrode and screen-printed electrode for caffeine sensor

Modified electrode[a]	Method[b]	Detection range (μM)	Limit of detection (μM)	Real sample	Sample volume (mL)	Sample treatment time (minutes)	Ref.
Cu-MOF/MWCNTs/SPCE	DPV	10–1500	7.9	Black coffee	—	—	53
MoO_3@GCNs/SPCE	DPV	0.5–359	0.021	Green tea and black coffee	—	10	54
CeO_2 NPs/SPE	DPV	5–476	2.4	Human blood	0.1	35	55
Zeolite/MWCNTs/carbon paste electrode	SWV	10–100	0.075	Beverage	—	—	48
Adenine-FSG/SPCE	SWV	1.1–340	0.59	Pharmaceutical drugs	—	—	33
Bare GCE	DPV	28–479	20	Energy drinks	20	3	56
Carbon black/graphene oxide/copper nanoparticle/PEDOT: PSS/GCE	SWV	11–64	3.4	Human serum and urine	—	—	25
Unmodified SPE	DPV	10–160	6.3	Pharmaceutical drugs	—	—	57
MWCNTs/Paper-based electrode	SWV	5–200	5	Commercial drinks	0.02	No required	This work

[a] Cu-MOF/MWCNTs/SPCE: copper metal organic framework, MWCNTs: multiwall carbon nanotubes, SPCE: screen-printed carbon electrode, MoO_3@GCNs: molybdenum trioxide grown on graphitic carbon nitride sheets, CeO_2NPs: cerium oxide nanoparticles, GCE: glassy carbon electrode, adenine-FSG: adenine-functionalized spongy graphene, PEDOT: PSS: poly(3,4-ethylenedioxythiphene) polystyrene sulfonate, SPE: screen-printed electrode. [b] DPV: differential pulse voltammetry; SWV: square-wave voltammetry.

Commercial beverages contain many interfering species; hence, tannic acid, ascorbic acid, glucose, sucrose and citric acid were used as potential interfering agents to examine the robustness of the developed sensor with respect to the effects of potential interfering agents. The SWV measurements at the paper-based sensor were performed in a phosphate solution (pH 1) containing caffeine and interference compounds. As shown in Fig. 9, the caffeine oxidation current was not significantly influenced by the interfering compounds at 1 : 1 interferent-to-caffeine ratio. The paper-based sensor responses stayed within the acceptable range event at 10 times higher interference concentration than caffeine, although the large error bars were observed (Fig. S9). These results were further supported by one-way ANOVA, which revealed no significant different in the current responses between caffeine alone and caffeine in the presence of interfering compounds.

3.4 Commercial beverage samples measurement

To evaluate the potential of the paper-based sensors for determination of caffeine in real samples, 11 commercial beverages including both caffeinated and non-caffeinated beverages (monster energy, black coffee – Georgia, Coca Cola, green tea – Oi ocha, Oolong tea – CGC, Oronamin C, decaffeinated coffee – UCC, Kokoa – Kikoma, salted lychee – Kirin, coffee latte – Georgia, and milk tea – Kirin) were selected as representative of real matrix. The beverage samples were obtained from a local supermarket in Japan. For each beverage, a sample (1 μL) was directly dropped into the phosphate solution (19 μL), and then SWV measurements were performed with three-times replication ($n = 3$). The performance of the paper-based sensor for the determination of caffeine in beverages was validated by comparing the results with those obtained by LC-MS. The results of the measurements are shown in Fig. 10 where the external calibration was used for the caffeine concentration determination in real sample. The caffeine concentration values obtained using the paper-based sensor were in good agreement with the caffeine concentration values determined by the LC-MS method for 9 out of 11 beverages. However, discrepancies were noted in the oolong tea and Coca-Cola samples which might be due to the matrix interference. As shown in Fig. S12, the agreement between the caffeine concentrations obtained by the paper-based sensor and LC-MS was significantly worse for coffee latte and milk tea. This result strongly indicates that the

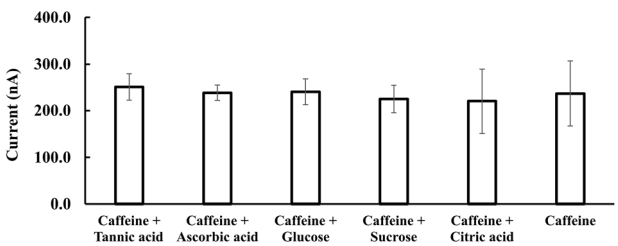

Fig. 9 Interference effect towards the oxidation of 0.1 mM caffeine in 0.1 M phosphate solution (interference: caffeine (1 : 1)). The reported error bars represented standard deviation from three independent measurements.

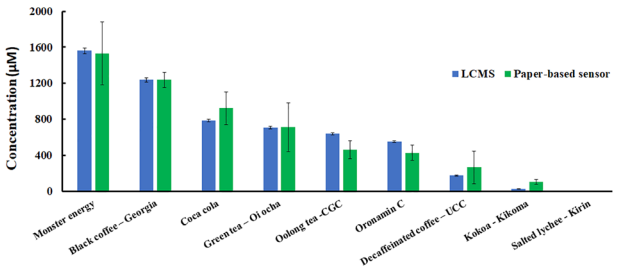

Fig. 10 Real sample measurement results obtained using the LC-MS method (blue) and the SWV method (green). The reported error bars represented standard deviation from three independent measurements.

paper-based sensor has a high potential for practical application in determination of caffeine concentrations in milk-free commercial beverages. By contrast, the significant difference between the levels of caffeine detected by the paper-based sensor and LC-MS in coffee latte and milk tea samples indicated that strong interference by compounds contained in milk degrades the reliability of the paper-based sensor for the determination of caffeine in these beverages. This interference was further investigated by mixing the monster energy drink, black coffee, and green tea with milk and non-fat milk in a ratio of 3 : 1. While good detection performance was obtained for mixtures with non-fat milk, the mixtures including milk fat showed poor determination accuracy. These results indicated that milk fat hinders accurate detection of caffeine by the paper-based sensor (Fig. S12), most likely due to the suspended fat matrix which limit the diffusion of caffeine into the carbon electrode surface.

4. Conclusion

In summary, the fabricated paper-based sensor was demonstrated to be suitable for detection of caffeine concentrations between 5 and 200 μM. The wax-modified paper and CNF film helped to confine the sample solution in the desired electrode area, enabling accurate and repeatable measurements. Based on the analysis of the caffeine diffusion coefficient and potential peak shift, the electrochemical oxidation of caffeine proceeded *via* a mechanism involving 2-protons and 4-electrons transfer processes, different from the 4-protons and 4-electrons processes discussed in previous studies. Furthermore, this work also demonstrated the suitability of paper-based sensors for practical application in direct detection of caffeine concentrations in commercial beverages, with the caffeine concentrations obtained using the paper-based sensor showing good agreement with the concentrations obtained with the LC-MS measurements. These results highlight the potential of paper-based sensors as simple, rapid, and practical platforms for caffeine analysis. However, the proposed paper-based sensor showed certain limitations when applied to milk containing sample, where fat interfered the electrochemical response. Future studies need to focus on the reduction of fat effect for caffeine detection in commercial beverages which can improve and extend practical application.

Author contributions

Muhammad Yudha Syahputra: data curation, formal analysis, investigation, methodology, review, and original draft. Erika Shinchi: resources, formal analysis, investigation and validation. Kenji Shida: resources, formal analysis, investigation, and validation. Masato Tominaga: conceptualisation, investigation, funding acquisition, writing – review, and supervision.

Conflicts of interest

There is no conflict to declare.

Data availability

The data supporting this article are included within the article and its supplementary information (SI). Supplementary information is available. See DOI: https://doi.org/10.1039/d6ra01066k.

Acknowledgements

MT acknowledges the grants from the Toshiaki Ogasawara Memorial Foundation for Science and Technology. This work was the result of using research equipment shared in the MEXT Project for Promoting the Public Utilization of Advanced Research Infrastructure (program for Supporting the Introduction of the New Sharing System; Grant no. JPMSX0422400025).

References

1 M. Fakioğlu and Y. Kalpaklı, *RSC Adv.*, 2022, **12**, 26504–26513.
2 S. Yamasaki, H. Kawasaki and Z. Cui, *Nutrients*, 2023, **15**, 1275.
3 A. Saimaiti, D.-D. Zhou, J. Li, R.-G. Xiong, R.-Y. Gan, S.-Y. Huang, A. Shang, C.-N. Zhao, H.-Y. Li and H.-B. Li, *Crit. Rev. Food Sci. Nutr.*, 2023, **63**, 9648–9666.
4 V. S. Reddy, S. Shiva, S. Manikantan and S. Ramakrishna, *Eur. J. Med. Chem. Rep.*, 2024, **10**, 100138.
5 D. M. B. Goldner, F. H. do Nascimento and J. C. Masini, *Sep. Sci. Plus*, 2024, **7**, e202400098.
6 C. Soto, H. D. Ponce-Rodríguez, J. Verdú-Andrés, R. Herráez-Hernández and P. Campíns-Falcó, *J. Chromatogr. A*, 2022, **1664**, 462770.
7 E. F. Göktaş, E. Kabil, L. Yatanaslan, E. Güneş and L. Dirikolu, *Biomed. Chromatogr.*, 2022, **36**, e5445.
8 M. Velička, E. Zacharovas, S. Adomavičiūtė and V. Šablinskas, *Spectrochim. Acta, Part A Mol. Biomol. Spectrosc.*, 2021, **246**, 118956.
9 B. Legas Muhammed, M. Hussen Seid and A. T. Habte, *Clin. Pharmacol.: Adv. Appl.*, 2021, **13**, 101–113.
10 Z. Wu, C. Li, H. Liu, T. Lin, L. Yi, D. Ren, Y. Gu and S. Wang, *J. Food Compos. Anal.*, 2024, **125**, 105793.
11 R. Singh, R. Gupta, D. Bansal, R. Bhateria and M. Sharma, *ACS Omega*, 2024, **9**, 7336–7356.
12 S. Singh, A. Glovi, G. Iula and S. Cinti, *ACS Electrochem.*, 2025, 5c00332.
13 J. Jose, V. Subramanian, S. Shaji and P. B. Sreeja, *Sci. Rep.*, 2021, **11**, 11662.
14 A. Geto and C. M. A. Brett, *Food Anal. Methods*, 2021, **14**, 2386–2394.
15 J. Arumugam, G. Shanmugam, M. Venkatesan and S. Sreedhar, *Mater. Chem. Phys.*, 2025, **339**, 130708.
16 S. Lisnund, V. Blay, K. Chansaenpak, J. Monkrathok and P. Pinyou, *ACS Omega*, 2025, **10**, 30717–30727.
17 S. Selvam, B. Balamuralitharan, S. N. Karthick, K. V. Hemalatha, K. Prabakar and H.-J. Kim, *Anal. Methods*, 2016, **8**, 7937–7943.
18 C. Hu, T.-R. Su, T.-J. Lin, C.-W. Chang and K.-L. Tung, *New J. Chem.*, 2018, **42**, 3999–4007.
19 J. I. Gowda and S. T. Nandibewoor, *Anal. Methods*, 2014, **6**, 5147.
20 C. Ferrag, M. Noroozifar and K. Kerman, *Mater. Sci. Eng. C*, 2020, **110**, 110568.
21 V. Sannasi, S. Kubendran and S. Prakash, *Diamond Relat. Mater.*, 2023, **136**, 110011.
22 Ž. Z. Tasić, M. B. Petrović Mihajlović, A. T. Simonović, M. B. Radovanović and M. M. Antonijević, *Sensors*, 2022, **22**, 9185.
23 A. Kushwaha, G. Singh, U. K. Gaur and M. Sharma, *Mater. Adv.*, 2024, **5**, 4378–4400.
24 R. M. S. Silva, A. M. Santos, A. Wong, O. Fatibello-Filho, F. C. Moraes and M. A. S. Farias, *Anal. Methods*, 2022, **14**, 3859–3866.
25 A. Wong, A. M. Santos, T. A. Silva and O. Fatibello-Filho, *Talanta*, 2018, **183**, 329–338.
26 R. Madhuvilakku and Y.-K. Yen, *J. Electroanal. Chem.*, 2022, **924**, 116882.
27 C. Van Der Horst, B. Silwana, E. Gil, E. Iwuoha and V. Somerset, *Electroanalysis*, 2020, **32**, 3098–3107.
28 N. A. Nia, M. M. Foroughi and S. Jahani, *Talanta*, 2021, **222**, 121563.
29 K. Y. Tajeu, E. Ymele, S. L. Zambou Jiokeng and I. K. Tonle, *Electroanalysis*, 2019, **31**, 350–356.
30 I. Sadok, K. Tyszczuk-Rotko and A. Nosal-Wiercińska, *Sensor. Actuator. B Chem.*, 2016, **235**, 263–272.
31 Y. Wang, X. Wei, F. Wang and M. Li, *Anal. Methods*, 2014, **6**, 7525–7531.
32 J. Wang, W. Wang, Y. An, L. Wu and Q. Zhang, *Microchem. J.*, 2024, **201**, 110574.
33 M. A. Mohamed, D. M. El-Gendy, N. Ahmed, C. E. Banks and N. K. Allam, *Biosens. Bioelectron.*, 2018, **101**, 90–95.
34 B. Mekassa, M. Tessema and B. S. Chandravanshi, *Sens. Biosens. Res.*, 2017, **16**, 46–54.
35 N. A. Aschemacher, S. A. Gegenschatz, C. M. Teglia, Á. S. Siano, F. A. Gutierrez and H. C. Goicoechea, *Talanta*, 2024, **267**, 125246.
36 Y. Wang, Y. Ding, L. Li and P. Hu, *Talanta*, 2018, **178**, 449–457.
37 W. Dungchai, O. Chailapakul and C. S. Henry, *Anal. Chem.*, 2009, **81**, 5821–5826.

38 Z. Nie, C. A. Nijhuis, J. Gong, X. Chen, A. Kumachev, A. W. Martinez, M. Narovlyansky and G. M. Whitesides, *Lab Chip*, 2010, **10**, 477–483.
39 L. Belcastro and F. Arduini, *Electrochim. Acta*, 2025, **541**, 147084.
40 R. Ding, Y. H. Cheong, A. Ahamed and G. Lisak, *Anal. Chem.*, 2021, **93**, 1880–1888.
41 S. Boonkaew, A. Yakoh, N. Chuaypen, P. Tangkijvanich, S. Rengpipat, W. Siangproh and O. Chailapakul, *Biosens. Bioelectron.*, 2021, **193**, 113543.
42 J. Jaewjaroenwattana, W. Phoolcharoen, E. Pasomsub, P. Teengam and O. Chailapakul, *Talanta*, 2023, **251**, 123783.
43 J. Lv, C. Li, S. Feng, S.-M. Chen, Y. Ding, C. Chen, Q. Hao, T.-H. Yang and W. Lei, *Ionics*, 2019, **25**, 4437–4445.
44 C. D. Rakhmania, Y. I. Azhar, K. Shida, E. Shinchi, T. Adachi, K. Sowa, Y. Kitazumi, O. Shirai and M. Tominaga, *Sens. Diagn.*, 2024, **3**, 1827–1834.
45 S. R. Sari, H. Sakaguchi, K. Shida, E. Shinchi, T. Adachi, K. Sowa, Y. Kitazumi, O. Shirai and M. Tominaga, *ACS Omega*, 2025, **10**, 47712–47713.
46 I. Streeter, G. G. Wildgoose, L. Shao and R. G. Compton, *Sensor. Actuator. B Chem.*, 2008, **133**, 462–466.
47 A. J. Jesu Amalraj, U. N. Murthy and S.-F. Wang, *J. Ind. Eng. Chem.*, 2022, **106**, 205–213.
48 S. M. Azab, M. Shehata and A. M. Fekry, *New J. Chem.*, 2019, **43**, 15359–15367.
49 D. L. O. Ramos, M. M. A. C. Ribeiro, R. A. A. Munoz and E. M. Richter, *J. Electroanal. Chem.*, 2022, **906**, 116006.
50 H. Lou, G. Hu, X. Luan, J. M. Steinbach-Rankins and M. J. Hageman, *J. Pharm. Sci.*, 2025, **114**, 256–264.
51 M. Vasilev, J. Suiter, D. Bohl and S. M. Thagard, *Chem. Eng. J.*, 2023, **473**, 144833.
52 W. E. Price, *J. Chem. Soc., Faraday Trans.*, 1989, **1**(85), 415.
53 M. Saraban, A. Numnuam, N. Nontipichet, T. Kangkamano, P. Thavarungkul, P. Kanatharana and S. Khumngern, *New J. Chem.*, 2024, **48**, 3638–3645.
54 G. Boopathy, M. Keerthi, S.-M. Chen, S. Meenakshi and M. J. Umapathy, *Mater. Chem. Phys.*, 2021, **269**, 124735.
55 M. Khairy, B. G. Mahmoud and C. E. Banks, *Sensor. Actuator. B Chem.*, 2018, **259**, 142–154.
56 L. Redivo, M. Stredanský, E. De Angelis, L. Navarini, M. Resmini and Ľ. Švorc, *R. Soc. Open Sci.*, 2018, **5**, 172146.
57 B. G. Mahmoud, M. J. A. Abualreish, M. Ismael and M. Khairy, *Anal. Methods*, 2024, **16**, 3993–4001.